

Fixed Points of the Dissipative Hofstadter Model

E. Novais,^{1,2} F. Guinea,^{1,3} and A. H. Castro Neto¹

¹*Department of Physics, Boston University, Boston, MA, 02215*

²*Department of Physics, Duke University, Durham, NC, 27708*

³*Instituto de Ciencia de Materiales de Madrid, CSIC, E-28049 Madrid, Spain.*

(Dated: November 20, 2018)

The phase diagram of a dissipative particle in a periodic potential and a magnetic field is studied in the weak barrier limit and in the tight-binding regime. For the case of half flux per plaquette, and for a wide range of values of the dissipation, the physics of the model is determined by a non trivial fixed point. A combination of exact and variational results is used to characterize this fixed point. Finally, it is also argued that there is an intermediate energy scale that separates the weak coupling physics from the tight-binding solution.

PACS numbers: 03.65.Yz, 03.75.Lm

Introduction A quantum particle interacting with an environment with a macroscopic number of degrees of freedom, the Caldeira-Leggett (CL) model [1], is one of the simplest models used in the study of decoherence in quantum systems. This model has been generalized to include the motion of a dissipative particle in a periodic potential [2], in a finite magnetic field [3], and in a combination of both situations [4]. The problem described by such a model applies to a large number of situations in condensed matter, quantum computation, and string theory. A few examples are: flux qubit dephasing in quantum computers [5], defects in Luttinger liquids [6], junctions between many Luttinger liquids [7], and non-trivial backgrounds in open string theory [4]. The CL model is also relevant to the study of the dephasing induced in mesoscopic systems by external gates [8, 9], and it always reproduces the short time dynamics of particles interacting with ohmic environments [10]. The model also describes the quantum motion of a vortex in a lattice. This model has attracted interest in the study of d-wave superconductors with strong phase fluctuations [11]. Note that, in this context, dissipation due to low energy modes arises naturally.

Although the phase diagram of a dissipative particle in a periodic potential is well understood [12, 13], there is no similar degree of understanding when a magnetic field is also added to the problem [4, 14]. This model became known as the dissipative Hofstadter model, and in the present work we analyze its phase diagram with a square lattice symmetry, the renormalization group (RG) flows and fixed points. We use mappings into spin and fermion Hamiltonians, and variational methods in order to obtain further information on the phase diagram, which, as discussed below, presents a number of new features with respect to the model without a magnetic field.

The model. In the absence of dissipation, the Hofstadter problem has a complex energy spectrum [15]. The model has a duality between the weak coupling and tight binding limits of the periodic potential [16] and, in both cases, the spectrum can be described by Harper's equa-

tion [17]. A similar duality holds in the dissipative case [4], which admits further extensions (see below).

We start by considering the limit where the periodic potential is weak. It was shown in Ref. [4] that from perturbation theory on the lowest Landau's levels the dissipative model can be described by a boundary conformal field theory in (1 + 1) dimensions with action (we use units such that $\hbar = 1 = k_B$),

$$S = \frac{\alpha}{4\pi} \sum_{\mu=x,\tau,i=1,2} \int_{-\infty}^{\infty} d\tau \int_0^{\infty} dx (\partial_{\mu}\Theta_i(x,\tau))^2 + \int_{-\infty}^{\infty} d\tau \left\{ i \frac{\beta}{4\pi} \sum_{i,j} \epsilon_{i,j} \Theta_i(0,\tau) \partial_{\tau}\Theta_j(0,\tau) + \lambda \sum_{i=1,2} \cos[\Theta_i(0,\tau)] \right\}, \quad (1)$$

where ϵ_{ij} is the totally anti-symmetric tensor. The particle's coordinates are represented by the boundary degrees of freedom of the field, $\vec{\mathbf{R}}(\tau) = \Theta_1(0,\tau)\hat{e}_x + \Theta_2(0,\tau)\hat{e}_y$. In addition, the particle moves in a periodic potential of lattice spacing a and amplitude λ ($\lambda = V/\Lambda \ll 1$, where V is the potential strength, and Λ is a high energy cut-off), and is subject to a perpendicular magnetic field of amplitude $\beta = Ba^2/\Phi_0$ (where Φ_0 is flux quantum). Dissipation arises from the first term in the r.h.s. of Eq. (1) when the bulk modes ($\Theta_i(x,\tau)$ with $x > 0$) are traced out. The dissipation strength is given by $\alpha = \eta a^2$ (where η is the dissipation coefficient).

In the absence of the potential the theory is Gaussian and the field propagator reads [4, 7, 14]

$$\langle \Theta_i(0,\tau) \Theta_j(0,0) \rangle_0 = 2\tilde{\alpha} \ln|\tau| \delta_{i,j} + i\pi\tilde{\beta} \operatorname{sgn}(\tau) \epsilon_{i,j}, \quad (2)$$

where $\tilde{\alpha} = \alpha/(\alpha^2 + \beta^2)$ and $\tilde{\beta} = \beta/(\alpha^2 + \beta^2)$. The first term in Eq. (2) is the well studied logarithmic correlations. The second part of the propagator is the Aharonov-Bohm phase that the particle picks due to the magnetic field. Using this result, it is simple to write the

partition function as an expansion in powers of λ

$$\mathbf{Z} = \sum_n \sum_{i_n=x,y} \sum_{\pm} \lambda^n \int_0^\beta d\tau_1 \int_0^{\tau_1} d\tau_2 \cdots \int_0^{\tau_{n-1}} d\tau_n \left\langle \hat{A}_{i_1}^\pm(\tau_1) \hat{A}_{i_2}^\pm(\tau_2) \cdots \hat{A}_{i_n}^\pm(\tau_n) \right\rangle_0, \quad (3)$$

where $A^\pm(\tau_i) = e^{\pm i\Theta_i(0,\tau_i)}$. Eq. (3) has a simple physical interpretation: each insertion of \hat{A}^\pm represents a jump of the center of the particle's Landau orbit by a vector of the "dual" lattice $\vec{r}_{m,n} = ma/\sqrt{\alpha^2 + \beta^2}\hat{e}_x + na/\sqrt{\alpha^2 + \beta^2}\hat{e}_y$ (n and m are integers) [14]. Which, for $\alpha = 0$ is a distance proportional to the Larmor radius ($\omega_c^{-1/2} = \beta^{-1/2}a$).

The complementary limit to the physics of Eq. (1) is to consider very large barriers. Thus, instead of the lowest Landau orbits, a tight binding approximation to the spectrum in the absence of dissipation is natural starting point[2, 4]. The partition function is now expanded in powers of the nearest neighbor hopping amplitude, t , between the minima of the periodic potential. The result is identical to Eq. (3) with the substitutions of Table I.

	Ω	g	$1/q$
weak barriers	$\lambda = V/\Lambda$	$\tilde{\alpha}$	$\tilde{\beta}$
tight binding	$\tilde{t} = t/\Lambda$	α	β

TABLE I: Duality relations between the strong and weak coupling limits of the dissipative Hofstadter model.

In the following, we focus on a cross section of the phase diagram, $\tilde{\beta}$ or $\beta = 1/q$ with $q \in \mathbb{Z}$, that contains most of the interesting features. We found convenient to re-write the problem in a unified Hamiltonian formalism

$$\mathcal{H} = \frac{v_s}{2} \int_0^\infty dz \left\{ \frac{1}{2g} [\partial_z \theta_{x,y}(z)]^2 + 2g [\Pi_{x,y}(z)]^2 \right\} + \Lambda \Omega \mathcal{T}_x e^{i\theta_x(0)} + \Lambda \Omega \mathcal{T}_y e^{i\theta_y(0)} + \text{h.c.}, \quad (4)$$

where we set $v = 1$, $[\theta_{x,y}(z_1), \Pi_{x,y}(z_2)] = \delta_{x,y} \delta(z_1 - z_2)$ and $\mathcal{T}_{x,y}$ are p-dimensional matrices ($\mathcal{T}_{x,y}^{-1} = \mathcal{T}_{x,y}^\dagger$) that satisfy the algebra

$$\mathcal{T}_x \mathcal{T}_y = e^{2\pi i/q} \mathcal{T}_y \mathcal{T}_x. \quad (5)$$

The correspondence between the parameters of Eq. (4) and the dissipative model are summarize on Table I. The stability of the both limits is given by the lowest order renormalization group (RG) equation

$$\partial_\ell \Omega = (1 - g)\Omega, \quad (6)$$

where $d\ell = d\Lambda/\Lambda$. Since the scaling dimension of $\Omega(\ell)$ in the strong coupling case is not the inverse of the one at weak coupling, there are values of (α, β) where both λ and \tilde{t} have runaway flows. This is similar to the case considered in Ref. [18, 19], where it was shown that a

particle in a triangular lattice can have a non trivial fixed point at intermediate coupling.

Variational treatment. For $g < 1$, $\Omega(\ell)$ scales toward strong coupling. This usually suggests that the fields $\theta_{x,y}(0)$ become "pinned" at some value $\bar{\theta}_{x,y}(0)$. We can gain insight into this "pinned phase" using the Self-Consistent Harmonic Approximation (SCHA) [20]. This approximation replaces the original periodic potential by harmonic wells adjusted self-consistently. Within SCHA we replace the boundary term in Eq. (4) by

$$V_{\text{sc}} = \sum_{a=x,y} \frac{K_a [\theta_a(0) - \bar{\theta}_a]^2}{2} \langle 0 | T_a + T_a^{-1} | 0 \rangle$$

where K_x and K_y are variational parameters. The p-dimensional state $|0\rangle$ has also to be adjusted variationally, and $\bar{\theta}_{x,y} = \arg\langle 0 | T_{x,y} | 0 \rangle$.

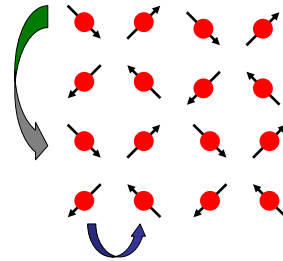


FIG. 1: Set of degenerate minima obtained using the SCHA for $q = 2$. The arrows denote the orientation of the state $|m, n\rangle$ for $m, n = 1, 2$. Possible hopping terms between these minima are also sketched.

Because of the periodicity of the potential, states $|n\rangle$ such that $\langle n | T_{x,y} | n \rangle$ differ by a phase, have the same ground state energy. It can be shown that the lowest energy is obtained for $|\langle 0 | \mathcal{T}_x | 0 \rangle| = |\langle 0 | \mathcal{T}_y | 0 \rangle| = \mathcal{T}$ and

$$K_x = K_y = \Lambda \Omega \mathcal{T} (\Omega \mathcal{T})^{\frac{1}{g-1}}. \quad (7)$$

Given a state $|0\rangle$, and using the relations in Eq. (5), we can construct p^2 states, $|m, n\rangle = T_x^m T_y^n |0\rangle$, $m, n = 1, \dots, p-1$ that lead to the same energy. Thus, the SCHA leads to a degenerate set of states labeled by the minimum in the periodic potential. The situation is illustrated in Fig.[1], where the case $q = 2$ is shown. The scaling dimension of the hopping between minima in the sublattice defined by a given vector $|m, n\rangle$ is $1/g$. Although tunneling is also possible between minima in different sublattices, it is reduced by the overlap factor $|\langle m, n | m', n' \rangle|$. These minima are closer in real space, and their scaling dimension is $1/(4g)$. Hence, for $1/4 < g < 1$ both the weak and strong coupling limits are unstable further supporting the existence of an intermediate fixed point. For a general value of $\tilde{\beta}$ (or $\beta = 1/p$) this result generalize to $1/p^2 < g < 1$. Moreover, the overlap of the states $|m, n\rangle$ define an effective Berry's phase generated when moving around each plaquette. It is easy

to show that the flux per plaquette needed to generate this Berry's phase is p . Hence, within the SCHA the weak barrier problem has an additional duality property, which leaves $\tilde{\beta}$ (β) unchanged, but replaces $g \leftrightarrow 1/(p^2g)$.

Mapping to a spin chain for $q = 2$. For $\tilde{\beta} = 1/2$ in the weak coupling case, or $\beta = 1/2$ in the tight binding limit, the operators T_x and T_y in Eq. (4) reduce to Pauli matrices, σ_x, σ_y . This equivalence suggests the use of a spin Hamiltonian with the same universal properties for the environment. Thus we replace Eq. (4) by two semi-infinite XXZ chains

$$\begin{aligned} \mathcal{H} = & \sum_{n \neq -1, 0} \sigma_n^x \sigma_{n+1}^x + \sigma_n^y \sigma_{n+1}^y + \Delta \sigma_n^z \sigma_{n+1}^z \\ & + v_s \Omega (\sigma_{-1}^x \sigma_0^x + \sigma_0^y \sigma_1^y) \end{aligned} \quad (8)$$

where $\Delta = \cos[\pi(1-g)]$ and $v_s = \pi |\sin(\pi g)| / (\pi + 2 \arcsin[\cos(\pi g)])$.

The spin Hamiltonian provides a different perspective of the infinite coupling limit studied by SCHA. As $\Omega \rightarrow \infty$, the low energy sector tends towards the tensor product of two semi-infinite chains (starting from sites ± 2) plus the low energy excitations of the three strongly coupled spins at sites $-1, 0$ and 1 . As the SCHA suggested, there are four degenerate states (see Fig. (1)). When we consider $\Omega < \infty$, the interaction between sites ± 2 and ± 1 can be treated as a perturbation of order $1/\Omega$ and the degeneracy is lifted to a doublet. In fact, this doublet is protected by a hidden symmetry (see below). After defining dual spin variables[21], $\tau_n^x = \sigma_n^x \sigma_{n+1}^x$ and $\tau_n^z = \prod_{j \leq n} \sigma_j^y$, we find that $[\tau_0^z, \mathcal{H}] = 0$. This conserved quantity is non-local in the original spin (dissipative) problem, thus it corresponds to a topological charge.

We can further understand the intermediate fixed point by solving the ‘‘non-interacting’’ problem, $g = 1/2$. As a bonus to be solvable, it is also believed that this point separates four different phases in the (α, β) plane[4]. Using the dual spin variables, the Hamiltonian breaks into three independent parts,

$$\mathcal{H} = \sum_{n \neq 0} [\nu_n^x + \nu_{n-1}^z \nu_n^z] + \sum_n [\mu_n^x + \mu_n^z \mu_{n+1}^z] + \mathcal{V}, \quad (9)$$

with the definitions: $\mu_n^i = \tau_{2n}^i$, $\nu_n^i = \tau_{2n-1}^i$ and $\mathcal{V} = (v_s \Omega - 1) [\mu_0^x + \mu_{-1}^z \mu_0^z]$. Eq. (9) implies that the odd sites of the original chain are mapped into two semi-infinite quantum Ising chains with open boundary conditions. The even sites are mapped into a single quantum chain and an impurity term (\mathcal{V}). After fermionizing the three chains and taking the continuous limit, it is straightforward to show that \mathcal{V} is an irrelevant operator of dimension 2. Hence, the *manifestly* conformal invariant RG fixed point is $v_s \Omega = 1$. In the fermionic language, the conservation of the topological charge is represented by a single Majorana fermion localized at the origin. In addition, we just showed that for $g = 1/2$ the fixed point is the resonance condition to a fermionic channel. Since

$\dim \mathcal{V} = 2$ at the ‘‘non-interacting’’ point, it is very likely that \mathcal{V} will also be an irrelevant operator for other values g . Eventually, as we consider $g \rightarrow 1$, the repulsive interaction between fermions became sufficiently strong to close the fermionic channel through the localization of a second Majorana ($\Omega \rightarrow 0$ fixed point).

The correspondence with the SCHA give us as simple picture about the particles mobility. In SCHA, the four minima of the potential are organized in sub-lattices depicted in Fig. (1). With the mapping to the spin chain, they can also be classified accordingly to the two possible values of the topological charge (τ_0^z). This fact suggests that at the intermediated fixed point the lattice breaks into two sub-lattices. Tunneling between minima of different sub-lattices does not occur, while the amplitude for wells in the same sub-lattice is given by the renormalized value of $1/\Omega$. This is very similar to the intermediated fixed point of a Brownian motion in a triangular lattice[19], where there are three geometrical sub-lattices. For intermediate values of dissipation, there is a regime where the particle avoids one of the sub-lattices, but moves on the other two. This scenario of an intermediated mobility can be further supported by noticing that for the exact solution, $g = 1/2$, the current operator also becomes quadratic in the fermion operators. Since the correlations will decay as τ^{-2} at long times, the particle mobility, $\mu_{ij} = \lim_{\omega \rightarrow 0} \omega \langle \Theta_i(0, \omega) \Theta_j(0, -\omega) \rangle$, is finite at the fixed point [22].

Fixed point at or near $g = 1$. When $\alpha, \tilde{\alpha} = 1$ the diagonal correlations between the $e^{i\theta_x(0)}$, $e^{i\theta_y(0)}$ operators decay as τ^{-2} . The RG equation can be derived in an $\epsilon = 1 - g$ [14, 23] expansion scheme,

$$\partial_\ell \Omega = \epsilon \Omega - C \sin^2(\pi/q) \Omega^3 + \mathcal{O}(\epsilon^2, \Omega^5), \quad (10)$$

where C is a constant of order unity. For $q = 2$, Eq. (10) implies a renormalized $\Omega \propto \sqrt{\epsilon}$. As $g \rightarrow 1$, this fixed point merge with the trivial $\Omega = 0$. The physical meaning of $\Omega = 0$ is straightforward when we look from the perspective of a quantum impurity problem. In Eq. (4), the two bosonic fields favor the localization of the spin variable along orthogonal directions. Thus, when $g = 1$, the ‘‘frustration’’ decouples the spin from the baths[24].

Phase diagram for half flux per unit cell. We now focus on a magnetic field which corresponds to half flux per plaquette, $\beta = 1/2$, which illustrates the different fixed points mentioned above. We summarize the discussion on Fig. (2).

In the tight binding limit, the particle is localized for $\alpha \geq 1$. Close to $\alpha \lesssim 1$ there is an intermediate fixed point, $\tilde{t}^* \propto \sqrt{1-\alpha}$. For $\alpha \approx 1/2$ the exact solution shows that $\tilde{t}^* \approx 1$. Finally, the duality transformation obtained by variational means indicates that a localized solution is unstable for $\alpha \geq 1/4$, so that an intermediate fixed point exists for $1/4 < \alpha < 1$.

In the weak barrier limit, except at $\alpha = 1/2$, the $\lambda = 0$ fixed point is unstable for all values of α . For $\alpha = 1/2$ the

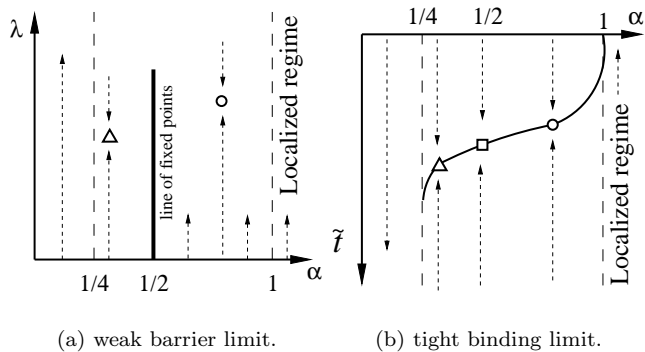


FIG. 2: Phase diagram of the dissipative Hofstadter model with half flux per unit cell, $\beta = 1/2$. The lines and symbols show the expected fixed points.

RG flow of λ is zero, leading to a line of fixed points [4]. This point in the phase diagram is equivalent to the well known line of fixed points of the model without the magnetic field[2]. This happens because as the particle hops in the “dual” lattice, \vec{r}' , it picks a phase of 2π around each plaquette. For $\alpha = \sqrt{3}/2$, the partition function is identical to the partition function in the tight-binding limit. Since the model is *self-dual* there ought to be at least one fixed point at intermediate coupling. For $\alpha = 1/(2\sqrt{3})$ we find $\tilde{\beta} = 3/2$. The model has the same properties as when $\tilde{\beta} = 1/2$, and the action, eq.(1), is formally equivalent to the action obtained in the tight binding limit. It seems likely that the fixed point obtained from the variational approach in this regime has the same properties as the one in the tight binding limit.

In the region $0 < \alpha < 1/4$ the weak and tight binding limits have RG flow towards strong coupling. The SCHA suggests that the particle is indeed delocalized with a phenomenology quite different from the $\lambda = 0$ fixed point. Instead of moving in the “dual” lattice, \vec{r}' , it freely moves in the lattice induced by the potential [25].

The existence of the self-dual point strongly suggests that for some parameters both the weak and the tight binding limits can be used to describe the model. However, at $\alpha = 1/2$ the different approaches lead to markedly different results. Similar discrepancies do exist in many other parts of the phase diagram. Hence, it is not obvious how to extrapolate the results from the weak barrier case to the tight binding limit and vice-versa. These differences between the weak barrier and tight binding limits are related to the range of validity of the field theories that describe each one. For instance, when the RG flow of the weak coupling case leads to energy scales of the order of $\max(\eta, \omega_c)$, Eq. (1) is no longer justified. Then, the theory must be supplemented with operators due to transitions to higher Landau levels. This is clear in the $\alpha = 1/2$ case, where the particle in the weak barrier limit effectively hops in a “dual” lattice with lattice

parameter $\sqrt{2}a$. Hence, starting from Eq. (1) it is not possible to account for the effects of the particle tunneling between minima of the periodic potential separated by a . This means that at a certain energy scale the line of fixed points stops, and the problem starts to renormalize to the exact solution that we discussed in the text. Conversely, using the duality properties of the model, there are other regions of the phase diagram where the tight binding suffers by the same problem.

In conclusion, we studied the dissipative Hofstadter model using scaling, exact results, and a variational approach. This allowed us to characterize the intermediate coupling fixed point of the model. Finally, we showed that results obtained in weak barrier or tight binding limits cannot be straightforwardly connected.

One of us (F. G.) is thankful to the Quantum Condensed Matter Visitor’s Program at Boston University. A.H.C.N. was partially supported through NSF grant DMR-0343790.

-
- [1] A. O. Caldeira and A. Leggett, *Ann. Phys.* **149**, 374 (1983).
 - [2] A. Schmid, *Phys. Rev. Lett.* **51**, 1506 (1983).
 - [3] S. Dattagupta and J. Singh, *Phys. Rev. Lett.* **79**, 961 (1997).
 - [4] C. Callan and D. Freed, *Nucl. Phys. B* **374**, 543 (1992).
 - [5] M. Grajcar *et al.*, (2004), *cond-mat/0501085*.
 - [6] C. L. Kane and M. P. A. Fisher, *Phys. Rev. B* **46**, 15233 (1992).
 - [7] C. Chamon, M. Oshikawa, and I. Affleck, *Phys. Rev. Lett.* **91**, 206404 (2003).
 - [8] F. Guinea, R. A. Jalabert, and F. Sols, *Phys. Rev. B* **70**, 085310 (2004).
 - [9] F. Guinea, *Phys. Rev. B* **71**, 045424 (2005).
 - [10] F. Guinea, *Phys. Rev. B* **67**, 045103 (2003).
 - [11] L. Balents *et al.*, (2004), *cond-mat/0408329*.
 - [12] S. Bulgadaev, *Pis'ma Zh. Eksp. Teor. Fiz.* **39**, 264 (1984), *JETP Lett.* **39**, 315 (1984).
 - [13] F. Guinea, V. Hakim, and A. Muramatsu, *Phys. Rev. Lett.* **54**, 263 (1985).
 - [14] C. G. Callan, A. G. Felce, and D. E. Freed, *Nucl. Phys. B* **392**, 551 (1993).
 - [15] D. Hofstadter, *Phys. Rev. B* **14**, 2239 (1976).
 - [16] D. Langbein, *Phys. Rev.* **180**, 633 (1969).
 - [17] P. G. Harper, *Proc. Phys. Soc. London* **68**, 874 (1955).
 - [18] H. Yi and C. L. Kane, *Phys. Rev. B* **57**, R5579 (1998).
 - [19] I. Affleck, M. Oshikawa, and H. Saleur, *Nucl. Phys. B* **594**, 535 (2001).
 - [20] G. Gómez-Santos, *Phys. Rev. Lett.* **76**, 4223 (1996).
 - [21] F. Guinea, *Phys. Rev. B* **32**, 7518 (1985).
 - [22] E. Novais and F. Guinea and A. H. Castro Neto, unpublished.
 - [23] G. Zaránd and E. Demler, *Phys. Rev. B* **66**, 024427 (2002).
 - [24] A. H. C. Neto *et al.*, *Phys. Rev. Lett.* **91**, 096401 (2003).
 - [25] The conclusion that the particle is delocalized for this parameters is in agreement with Ref. [4].